HHS Public Access

Author manuscript

FASEB J. Author manuscript; available in PMC 2021 February 01.

Published in final edited form as:

FASEB J. 2020 February ; 34(2): 3399–3412. doi:10.1096/fj.201902117R.

Knee loading repairs osteoporotic osteoarthritis by relieving abnormal remodeling of subchondral bone via Wnt/β-catenin signaling

Weiwei Zheng[1], **Beibei Ding**[1], **Xinle Li**[1,2], **Daquan Liu**[1,2], **Hiroki Yokota**[3], **Ping Zhang**[1,2,3,4,#]

[1.]Department of Anatomy and Histology, School of Basic Medical Sciences, Tianjin Medical University, Tianjin 300070, China

[2.]Key Laboratory of Hormones and Development (Ministry of Health), Tianjin Key Laboratory of Metabolic Diseases, Tianjin Medical University, Tianjin 300070, China

[3.]Department of Biomedical Engineering, Indiana University-Purdue University Indianapolis, IN 46202, USA

[4.]Tianjin Key Laboratory of Spine and Spinal Cord, Tianjin Medical University, Tianjin 300052, China

Abstract

Osteoporotic osteoarthritis (OPOA) is a common bone disease mostly in the elderly, but the relationship between OP and OA is complex. It has been shown that knee loading can mitigate OA symptoms. However, its effects on OPOA remain unclear. In this study, we characterized pathological linkage of OP to OA, and evaluated the effect of knee loading on OPOA. We employed two mouse models (OA and OPOA), and conducted histology, cytology, and molecular analyses. In the OA and OPOA groups, articular cartilage was degenerated and OARSI score was increased. Subchondral bone underwent abnormal remodeling, the differentiation of BMSCs to osteoblasts and chondrocytes was reduced, and migration and adhesion of pre-osteoclasts were enhanced. Compared to the OA group, the pathological changes of OA in the OPOA group were considerably aggravated. After knee loading, however, cartilage degradation was effectively prevented, and the abnormal remodeling of subchondral bone was significantly inhibited. The differentiation of BMSCs was also improved, and the expression of Wnt/β-catenin was elevated. Collectively, this study demonstrates that osteoporosis aggravates OA symptoms. Knee loading restores OPOA by regulating subchondral bone remodeling, and may provide an effective method for repairing OPOA.

[#] Corresponding Author: Ping Zhang, MD, Department of Anatomy and Histology, School of Basic Medical Sciences, Tianjin Medical University, 22 Qixiangtai Road, Tianjin 300070, China, Phone: 86-22-83336818, Fax: 86-22-83336810, pizhang@tmu.edu.cn.

AUTHOR CONTRIBUTIONS

W. Zheng and P. Zhang designed research; W. Zheng, B. Ding and X. Li conducted research; W. Zheng, B. Ding, D. Liu and X. Li collected the data; W. Zheng, B. Ding, H. Yokota and P. Zhang analyzed the data; W. Zheng and P. Zhang wrote the manuscript; P. Zhang approved the final manuscript as submitted; P. Zhang accepted responsibility for integrity of data analysis.

CONFLICT OF INTEREST

The authors declare that they have no conflict of interest.

Keywords

Osteoporotic osteoarthritis; Osteoblast; Osteoclast; Wnt signaling; Knee loading

INTRODUCTION

Osteoarthritis (OA) and osteoporosis (OP) are two common musculoskeletal disorders that cause disability and reduce the quality of life, especially in women after menopause (1). OA is usually regarded as a cartilage disease, but the pathological process includes changes in adjacent bone, synovium, ligaments, and tendons (2). OP is characterized by excessive bone resorption, micro architectural deterioration of bone tissue, and reduction in bone strength leads to an increase in fracture risk (3). Osteoporotic osteoarthritis (OPOA) is a special form of OA, and it is mainly associated with brittle subchondral bone and micro fracture, both of which accelerate OA progression (4, 5). So far, the relationship between OP and OA is not well understood. Some studies suggested vague association of OP to OA (6), while others reported the common pathogenic mechanism since excessive bone resorption, typical in OP, takes place in the early OA stage (7, 8). In our previous work, knee loading was effective in treating OP and OA separately, and thus we hypothesized that it may be effective in treating OPOA.

Subchondral bone can be divided into two anatomic entities: bone plate and trabecular bone. A subchondral bone plate is thin cortical bone under the calcified cartilage. Arising from subchondral bone plate is the supporting trabeculae, which comprise subchondral trabecular bone. Subchondral trabecular bone exerts important shock-absorbing and supportive functions in normal joints, and may also be useful for a nutrient supply to cartilage (9). Microstructural changes of subchondral bone can affect the integrity of articular cartilage and cause cartilage degeneration (10, 11). In addition, in the pathological process of OA and OP, there are changes in the microstructure of the subchondral bone (12, 13). Receptor activator of nuclear factor κB ligand (RANKL) is one of the most important molecules in bone remodeling. It was identified as a key signaling molecule for the differentiation of bone macrophages to mature osteoclasts, which lead to bone resorption (14). Cathepsin K (CTSK) is highly expressed in osteoclasts and is secreted in the bone-resorbing compartment (15). Runt-related transcription factor 2 (RUNX2) is an essential transcription factor for osteoblast differentiation and skeletal development. Alkaline phosphatase (ALP) is one of osteogenic marker genes. They are all up-regulated when bone formation is increased (16). Bone formation and bone resorption of subchondral bone directly affect subchondral bone microstructure.

Since bone is a mechano-sensitive organ, moderate pulsating loading, oscillatory compressive loads, can be applied to various synovial joints in a form of elbow loading, knee loading and ankle loading (17–20). Joint loading can change intramedullary pressure of bone cavities. The moderately changing pressure may generate fluid flow in a lacuna canalicular network in bone cortex, and activate anabolic genes in bone (18, 21). In our previous studies, we have shown that knee loading is effective in enhancing healing of bone wounds in a femur neck (22), promoting longitudinal bone growth (17), preventing bone loss in femoral

head necrosis (21), reducing bone loss in an OP mouse model (23), and preventing tissue degeneration in OA (24, 25). However, the role of knee loading on OPOA is unclear.

Canonical Wnt signaling is a crucial anabolic pathway in bone (26, 27). It is reported that activation of canonical Wnt signaling in osteoblasts increases bone mass, whereas inactivation results in a decrease in bone mass (28). Wnt3a and β-catenin are stimulators of Wnt signaling, and they regulate bone formation and resorption (28). Previous work by Lara-Castillo N et al. demonstrated that mechanical loading rapidly activates β-catenin signaling in osteocytes (29). Javaheri B et al. showed that mice with a heterozygous deletion of β-catenin in osteocytes lose the ability to form new bone in response to mechanical loading (30). Furthermore, our previous experiments showed that knee loading could inhibit osteoclast development by regulating Wnt signaling and be used to treat early OA (25), Wnt3a plays a key role in the treatment of OP in response to knee loading (23). However, whether knee loading also plays a role in OPOA by regulating Wnt signal is unknown.

We hypothesized that knee loading can regulate abnormal bone remodeling of subchondral bone in the early OPOA mouse model, thereby reducing the degradation of articular cartilage with a significant therapeutic effect on early OPOA via Wnt signaling. To test the hypothesis, we used a surgically induced mouse model of OPOA (OVX + OA surgery). To evaluate daily loading effects, we determined the degree of cartilage destruction using the Osteoarthritis Research Society International (OARSI) score, and we analyzed the alteration of cartilage and subchondral bone by histology with hematoxylin and eosin (H&E) and Safranin O staining. We also examined the expression of bone formation marker (ALP and RUNX2), bone resorption marker (CTSK and RANKL), and genes involved in canonical Wnt signaling (Wnt3a and β-catenin) in Western blot analysis. We also isolated bone marrow-derived cells to assay migration and adhesion of pre-osteoclasts, osteoblast differentiation and chondrogenesis.

MATERIALS AND METHODS

Animals and materials preparation

Eighty 16-week-old C57BL/6 female mice (Animal Center of Academy of Military Medical Sciences, China) were used. Four to five mice per cage were housed under pathogen-free conditions, and were fed with standard laboratory rodent chow and tap water ad libitum. Mice were housed in plastic cages at room temperature (25°C) with a 12-h light-and-dark cycle, and acclimatized for seven days before use. All experiments were conducted in accordance with the National Institutes of Health Guide for Care and Use of Laboratory Animals and approved by the Ethics Committee of the Tianjin Medical University.

Murine receptor activator of nuclear factor Kappa-B ligand (RANKL) and murine macrophage-colony stimulating factor (M-CSF) were purchased from PeproTech (Rocky Hills, NC, USA). An immunohistochemical staining kit and 3, 3′-diaminobenzidine (DAB) substrate kit were purchased from ZSGB-BIO (Beijing, China). Dulbecco's Modified Eagle's Medium (DMEM), Minimum Essential Medium Alpha (MEM-α), fetal bovine serum, penicillin, streptomycin and trypsin were purchased from Invitrogen (Carlsbad, CA,

USA). Other chemicals were purchased from Sigma (St. Louis, MO, USA) unless otherwise stated.

Experimental design

Mice were randomly divided into five groups with sixteen mice in each group. Group sham was designated the sham group. The OA group received OA surgery on both knees (31). Group OAL was designated the OA + Loading group and received OA surgery and loading on two knees. Group OPOA was designated the OA + OP group and received OA surgery and ovariectomy (32). Group OPOAL was designated the OA + OP + Loading. The knee loading was administered daily for 28 days, starting one day after OA (28 days after OVX), to enable estrogen-deficient osteopenia development. After BMD/BMC measurement, all animals were killed at 4 weeks after OA surgery.

Ovariectomy

The animals were anesthetized with 1.5% isoflurane (IsoFlo; Abbott Laboratories, North Chicago, IL, USA) at a flow rate of 1.0 L/min. We placed the mouse in prone position. The back was scrubbed and prepared in surgically sterile fashion. We made a midline dorsal skin incision using a scalpel and excised the bilateral ovaries with scissors (33).

OA surgery

Surgery was performed using a sterile technique and under anesthetic with 1.5% isoflurane (IsoFlo, Abbott Laboratories, North Chicago, IL, USA) at a flow rate of 1.0 L/min. The right hindlimb was shaved and sterilized with 70% alcohol solution prior to generation of a 20-mm incision to expose the right knee joint. The medial collateral ligament was transected and the articular cavity was opened to allow for removal of the medial meniscus from its anterior attachment to the tibia (24). The surgery site was washed with sterile saline to remove tissue debris, and the incision was closed. After finishing surgery on the right knee, the same procedure was conducted on the left knee.

In order to alleviate the pain associated with ovariectomy and OA surgery, the mouse was administered a dose of 0.05 mg/kg buprenorphine hydrochloride every 8 h for the first 3 postoperative days. After surgery, 1% pramoxine hydrochloride ointment was applied on the incision sites every day for the first 3 postoperative days. Buprinorphine hydrochloride was applied on the incision sites as analgesia after surgery.

Knee loading

The second day after OA surgery, loading was conducted to both knees using a custom-made loader for 4 weeks (25, 34). During a loading process, the mouse was mask-anesthetized using 1.5% isoflurane. Dynamic loads were sinusoidal at 1 N (peak-to-peak) and the frequency was 5 Hz for 6 min/day (each knee, 3 min). The loading device was calibrated using a load cell (Model LLB130, FUTEK Advanced Sensor Technology, Irvine, CA) to determine peak compressive force. To position the knee properly, the lower end of the loading rod and the upper end of the stator were designed to form a pair of semispherical cups. The lateral and medial epicondyles of the femur together with the lateral and medial condyles of the tibia were confined in the cups (Fig. 1*A*) (19). The tip of the loader was 5

mm in diameter. Three non-loaded groups (Sham, OA and OPOA) were given sham loading, in which mice were given anesthesia and placed on the loading device without any dynamic force. After finishing the right knee loading, the same loading procedure was conducted on the left knee. Femurs and tibias were collected from 6 mice per group, and bone marrow cells were isolated. The knee joint was collected from the remaining 10 mice per group, in which the right knee was used for histological analysis and the left knee for Western blot analysis.

Measurements of bone mineral density and bone mineral content

The mouse was mask-anesthetized using 1.5% isoflurane and placed on the platform in the prone position, and images were acquired in about 5 min. Bone mineral density (BMD, g/cm^2) and bone mineral content (BMC, mg) of the knee were measured by peripheral dual-energy X-ray absorptiometry (pDEXA) before sacrifice (22).

Histology, TRAP, MacNeal's and immunohistochemistry assays

After sacrifice, knee samples were fixed in 10% neutral buffered formalin for 48 h and decalcified in 14% ethylene diamine tetra-acetic acid (EDTA, pH 7.4) for 2 weeks. Decalcified samples were embedded in paraffin, and 5-μm-thick coronal sections were cut with a Leica RM2255 microtome (Leica Microsystems Inc., Bannockburn, IL). Tissue sections were stained with Safranin O and graded using an OA Research Society International (OARSI) score to assess histopathological grade of cartilage (35–38). The slides were then stained with hematoxylin and Eosin (H&E) for detecting the histological parameters of articular cartilage and subchondral bone. The images of the knee were captured with an Olympus BX53 microscope and tibia Olympus DP73 camera. Measurements were performed on the proximal side of the growth plate. We determined B.Ar/T.Ar (in %, T.Ar = total tissue area, and B.Ar = trabecular bone area, calculated from the total trabecular area), CC/TAC (ratio of calcified cartilage to the total articular cartilage), and SBP (subchondral bone plate) thickness (25). Additionally, we used tartrate resistant acid phosphatase (TRAP) staining to determine osteoclast development according to the standard protocol (Sigma). The ratio between length of TRAP-positive cells and total circumference of bone trabecula was calculated (23). It represented the activity of osteoclast. MacNeal's staining was used for identifying osteoblasts as described previously (39, 40).

Immunohistochemical staining was performed using an immunohistochemical kit and 3, 3-diaminobenzidine (DAB) substrate kit was used according to the manufacturer protocol. Knee sections were incubated with primary antibodies against Wnt3a (Abcam, Cambridge, MA, USA) and β-catenin (Cell Signaling, Danvers, MA, USA) overnight at 4°C. The ratio of the area stained by Wnt3a or β-catenin to the total field area was calculated in a blinded fashion (25).

Western blot analysis

Tissues were lysed in a radioimmunoprecipitation assay (RIPA) lysis buffer, containing protease inhibitors and phosphatase inhibitors (Roche Diagnostics GmbH, Mannheim, Germany). Isolated proteins were fractionated using 10% sodium dodecyl sulfate-polyacrylamide gels and electro-transferred to polyvinylidene difluoride membranes

(Millipore, Billerica, MA, USA). Primary antibodies specific to RUNX2, β-catenin (Cell Signaling, Danvers, MA, USA), Wnt3a (Abcam, Cambridge, MA, USA), ALP, RANKL (Proteintech, Wuhan, China) and β-actin were employed. After incubation with secondary IgG antibodies conjugated with horseradish peroxidase, signals were detected with enhanced chemiluminescence. Data were presented with reference to control intensities of β-actin (41).

Isolation of bone marrow-derived cells

After euthanasia, bone marrow-derived cells were collected by flushing the femur and tibia with Iscove's MEM (Gibco-Invitrogen, Carlsbad, CA, USA) with 2% fetal bovine serum (FBS). Cells were separated by low-density gradient centrifugation and cultured in α-MEM supplemented with 10% FBS (19, 31).

Migration and adhesion of pre-osteoclasts assays

Migration of pre-osteoclasts was evaluated using a transwell assay as described previously with minor modifications (42). Bone marrow-derived cells (2×10^6 cells/ml in 6-well plates) were cultured in MEM-α supplemented 10% FBS, 30 ng/ml M-CSF and 20 ng/ml RANKL for 4 days. The identified osteoclast precursor cells (1×10^5 cells/well) were loaded onto the upper chamber of transwells and allowed to migrate to the bottom chamber through an 8-μm polycarbonate filter coated with vitronectin (Takara Bio Inc., Otsu, Shiga, Japan). The medium in the upper chamber was replaced with free serum MEM-α, and the lower chamber contained MEM-α consisting of 1% bovine serum albumin (BSA) and 30 ng/ml M-CSF. After 6 h reaction, cells were stained with crystal violet, and the number of osteoclast precursor cells in the lower chamber (attached onto the bottom of the transwells) was counted. Five fields per well (200×) were randomly selected and photographed for counting.

For assaying adhesion, the identified osteoclast precursor cells (1×10^5 cells/well) were placed into 96-well plates coated with 5 mg/ml vitronectin and 30 ng/ml M-CSF as previously described (43, 44). After 30 min of incubation, cells were fixed with 4% paraformaldehyde at room temperature for 10–15 min and stained with crystal violet. The number of adherent cells was counted.

Osteoblast differentiation and chondrogenic assays

For osteoblast differentiation, cells were cultured at 2×10^6 cells/ml in 6-well plates consisting of the osteogenic differentiation medium (MesenCult proliferation kit, supplemented with 10 nM dexamethasone, 50 μg/ml ascorbic acid 2-phosphate, and 10 mM β-glycerophosphate) (43). The medium was changed every other day, and cells were cultured for 2 weeks. On day 14, cells were stained using an alkaline phosphatase (ALP) kit (Sigma-Aldrich, St. Louis, MO, USA). The percentage of ALP-positive colonies was determined.

For chondrogensis, bone marrow mononuclear cells were plated at 1×10^6 cells/ml in chondrogenic differentiation medium (MesenCult proliferation kit supplemented with 10^{-8} mol/l dexamethasone, 50 μg/ml ascorbic acid 2-phosphate, 10 mmol/l β-glycerophosphate

and 10 ng/ml TGFβ3) in 6-well plates for 4 weeks. The medium was changed every other day. Cells were fixed in 10% buffered formalin for 30 min at room temperature, washed with PBS, and incubated with 1% Alcian Blue in 0.1 M HCl (pH 1.0) for at least 2 h. Chondrogenic cells were visualized as blue-stained cells (45).

Statistical analysis

The data were expressed as mean ± standard error of mean (SEM) unless otherwise stated. For more than a 2-group comparison, one-way ANOVA was conducted followed by a post-hoc test using Fisher's protected least significant difference. For a 2-group comparison, Student's *t* test was conducted. All comparisons were two-tailed and statistical significance was assumed at $P < 0.05$. * = $P < 0.05$, ** = $P < 0.01$ and *** = $P < 0.001$ vs. the sham group; # = $P < 0.05$, ## = $P < 0.01$ and ### = $P < 0.001$; and & = $P < 0.05$, && = $P < 0.01$ and &&& = $P < 0.001$.

RESULTS

All animals tolerated the procedures, and no bruising or tissue damage was detected at the surgery site.

Knee loading decreased body weight of OVX mice

We first evaluated body weight. No significant difference of starting body weight was detected among the groups, but compared to the sham group, the OPOA group showed a significant increase in body weight ($P < 0.001$). Knee loading reduced the elevated body weight of OVX mice ($P < 0.001$; Fig. 1*B*, *C*).

Knee loading increased BMD and BMC *in vivo*

We next examined any changes in BMD and BMC. Compared to the sham control, the OA and OPOA groups presented a significant reduction in BMD and BMC in the knee (all $P < 0.01$). Furthermore, compared to the OA group, the OPOA group showed a marked decrease in BMD and BMC. However, four-week application of knee loading suppressed this reduction. Therefore, the loaded OA and OPOA mice increased BMD and BMC in the knee (all $P < 0.05$; Fig. 1*D*, *E*). The data were expressed with standard deviation (SD).

Knee loading reduced abnormal bone reconstruction of subchondral bone in the OA and OPOA groups

The primary aim in this study is the effect of knee loading on subchondral bone and cartilage. Thickness of SBP was measured using H&E-stained sections (Fig. 2*A*, *B*) to evaluate changes in subchondral bone. Compared to the sham group, those in OA and OPOA group showed thinner SBP (both $P < 0.001$). After knee loading, thickness of SBP was increased in the OAL and OPOAL group (both $P < 0.01$; Fig. 2*D*). The data were expressed with standard deviation (SD).

To evaluate a volume fraction of subchondral bone, B.Ar/T.Ar ratio was detected by H&E staining (Fig. 2*A*, *B*). The OA and OPOA groups exhibited a lower B.Ar/T.Ar ratio compared to the sham group (both $P < 0.001$), and knee loading presented a significant

recovery of B.Ar/T.Ar (both $P < 0.05$; Fig. 2*E*). The data were expressed with standard deviation (SD).

There was no significant change in subchondral cortical bone SBP between the OPOA and OA groups (Fig. 2*F*). However, there was a significant reduction of the cancellous bone (B.Ar/T.Ar) in the OPOA group ($P < 0.05$; Fig. 2*G*).

Histological parameters of trabecular bone on the proximal side of the growth plate in the proximal tibia were determined by H&E staining. Trabecular bones were indicated by the arrows (Fig. 2*C*). The OVX mice exhibited a significant decrease in B.Ar/T.Ar ($P < 0.05$; Fig. 2*H*). However, there was no significant change between the sham and OA groups. Furthermore, knee loading presented significant recovery of B.Ar/T.Ar in the OPOAL group ($P < 0.01$; Fig. 2*H*).

Knee loading inhibited osteoclastogenesis

So far, we show the benefits of knee loading on OA and OPOA. Hereafter, we evaluated the effects of knee loading on cellular differentiation and molecular signaling. To investigate whether knee loading affected bone resorption in OA and OPOA *in vivo*, we conducted TRAP staining (Fig. 3*A*, *B*). The osteoclast surface (%) was increased in the OA and OPOA groups (both $P < 0.001$), while this increase was suppressed in the OAL and OPOAL groups (both $P < 0.01$; Fig. 3*E*).

To evaluate whether knee loading affected osteoclast functions in OA and OPOA *in vitro*, we performed migration (Fig. 3*C*) and adhesion assays (Fig. 3*D*). In the OA and OPOA group, migration and adhesion of pre-osteoclasts were stimulated compared to the sham group (all $P < 0.01$). Those activities were significantly reduced in the loading-treated group (all $P < 0.05$; Fig. 3*F*, *G*).

We also examined the expression of RANKL and CTSK in the left knee. In the OA and OPOA groups, the levels of RANKL and CTSK were significantly increased compared to the sham control group (all $P < 0.05$), and they were suppressed by knee loading in the OAL and OPOAL groups (all $P < 0.05$; Fig. 3*H*–*J*).

Knee loading promoted osteoblast differentiation

We employed MacNeal's staining *in vivo* (Fig. 4*A*) and ALP staining *in vitro* (Fig. 4*B*) to evaluate the differentiation of osteoblasts from mesenchymal stem cells. The number of osteoblasts in the OA and OPOA groups were significantly decreased compared to the sham control group (both $P < 0.001$; Fig. 4*C*, *D*). However, the numbers were significantly increased in the knee loading-treated group (all $P < 0.01$; Fig. 4*C*, *D*).

We also examined expression of ALP and RUNX2 in the knee joint. In the OA and OPOA groups, the levels of ALP and RUNX2 were significantly decreased compared to the sham control group (all $P < 0.05$), and they were restored by knee loading in the OAL and OPOAL groups (all $P < 0.05$; Fig. 4*E*–*G*).

Knee loading decreased articular cartilage degradation and increased the number of chondrocytes

Safranin O staining showed that cartilage surface was smooth and intact in the sham control group. However, the OA and OPOA groups exhibited massive proteoglycan loss and apparent hypocellularity in 4 weeks after OA induction (Fig. 5*A*, *B*). In the OA and OPOA groups, OARSI scores revealed significant degeneration of the articular cartilage compared to the sham control group (both $P < 0.001$). Moreover, the OPOA group had a lower OARSI scores than the OA group ($P < 0.05$). Application of knee loading significantly improved OARSI scores both in the OAL and OPOAL groups (both $P < 0.001$; Fig. 5*C*).

We counted the number of chondrocytes and the number of vacuolar cells (black one-way arrows) in the area adjacent to subchondral bone of the medial tibial plateau with Safranin O staining (Fig. 5*B*). The number of chondrocytes in the OA and OPOA groups were significantly decreased compared to the sham control group (both $P < 0.001$). After knee loading, however, the number of chondrocytes was increased in the OAL and OPOAL groups ($P < 0.01$ and $P < 0.001$; Fig. 5*D*). In contrast, the number of vacuolar cells in two model groups were increased compared to the sham control group (both $P < 0.001$). Quantities of these cells were decreased after application of knee loading in the OAL and OPOAL groups ($P < 0.001$ and $P < 0.05$; Fig. 5*E*).

Both in the OA and OPOA groups, thickness of the calcified cartilage (CC) (black two-way arrows) increased whereas that of hyaline cartilage (HC) (black two-way arrows) decreased with a tidemark moving towards the articular surface. The calcified cartilage thickness was decreased by knee loading (Fig. 5*B*). Notably, the value of CC/TAC in the OA and OPOA groups were higher than that in the sham control group (both $P < 0.001$). The value of CC/TAC was significantly decreased by knee loading in the OAL and OPOAL groups (both $P < 0.001$; Fig. 5*F*).

Furthermore, we performed a chondrocyte differentiation assay using bone marrow-derived mesenchymal cells (Fig. 5*G*, *H*). We employed approximately the same number of MSCs in each group, and chondrogenic cells were visualized as blue-stained cells. The number of differentiated chondrocytes derived from the OA and OPOA groups were significantly decreased compared to the sham control group (both $P < 0.001$). However, the number of differentiated chondrocytes derived from OAL and OPOAL mice revealed a significant restoration ($P < 0.001$ and $P < 0.05$).

Knee loading increased the expression of Wnt3a and β-catenin

To evaluate any change in Wnt/β-catenin signaling in response to knee loading in the OA and OPOA groups, we examined the expression of Wnt3a and β-catenin in the knee joint. Immunohistochemistry analysis showed that compared to the sham group, the positive cells of Wnt3a and β-catenin in the OA and OPOA groups were significantly decreased (all $P < 0.001$). However, those positive cells were increased by knee loading (all $P < 0.05$; Fig. 6*A*–*D*).

Western blot analysis showed that compared to the sham group, the expression of Wnt3a and β-catenin in the OA and OPOA groups were significantly decreased (all $P < 0.05$). However, their levels were restored by knee loading (all $P < 0.05$; Fig. 6*E*–*G*).

DISCUSSION

The current study demonstrates that knee loading is able to delay the degradation of articular cartilage by inhibiting subchondral bone reconstruction in a mouse model of OPOA, and Wnt3a-mediated signaling is involved in the response to knee loading. The result shows that OP increases the severity of cartilage damage in the knee of OA mice, and the pathological damage in the OPOA group was severer than that of the OA group. The major differences included changes in subchondral bone mass and pathological changes in articular cartilage. To further evaluate loading effects, BMD, SBP and CC/TAC were determined. A 4-week application of daily knee loading significantly suppressed OVX-induced reduction in BMD, SBP and CC/TAC. Consistent with those observed effects, the loaded mice exhibited a significant increase in bone mass and reduction in the extent of cartilage destruction. Furthermore, knee loading increased the number of osteoblasts and elevated the expression of RUNX2 and ALP. Knee loading also suppressed bone resorption as well as the level of osteoclast markers such as CTSK and RANKL. Abnormal bone remodeling of subchondral bone plays a key role in OPOA, and knee loading may inhibit the reconstruction of subchondral bone through Wnt signaling, thereby delaying the degradation of articular cartilage. In addition, knee loading can repair articular cartilage damage (Fig. 7).

While OP and OA are the most prevalent skeletal diseases related to age, the relationship between these diseases is complex (7). Some studies reported an inverse relation between bone density and bone turnover in patients with OP and OA (5, 46, 47), and others reported that they might share the same pathogenic mechanism, since excessive bone resorption takes place in the early stage of OA (6–8). OP and OA in the early stages often present subchondral microfractures or microstructural destruction (47). Subchondral microfractures and subchondral bone remodeling accelerate articular cartilage degeneration in the early OA (4). Thus, subchondral bone is a potential target for the treatment of early OPOA.

The Wnt/β-catenin signaling pathway is one of the pathways that are sensitive to mechanical loading (29, 30). It plays a critical role in bone homeostasis, in which Wnt3a and β-catenin are involved in both bone formation and resorption through osteoblasts and osteoclasts (28). We have previously shown that mechanical loading regulates the homeostasis of osteoblasts, osteoclasts and endothelial cells by regulating Wnt signaling and protects OP (23). In this study, we found that knee loading significantly increased the expression of Wnt3a and β-catenin in OA and OPOA mice. The result indicates that Wnt3a signaling is involved in the regulation of osteoblasts and osteoclasts in response to knee loading.

There is a close biomechanical relationship between articular cartilage and subchondral bone. Subchondral bone degeneration is usually associated with articular cartilage defects, and subchondral bone sclerosis together with progressive cartilage degeneration is widely recognized as a hallmark of OA (9). In addition, in the pathological process of OP and OA, there are changes in the microstructure of the subchondral bone (12, 13). Bone formation

and bone resorption of subchondral bone directly affect the changes of subchondral bone microstructure. Subchondral bone can be divided into two different anatomical entities: bone plate and trabecular bone (48). These two different anatomical structures are composed of cortical bone and cancellous bone, respectively (49). In OPOA, there are different changes in the bones of these two structures.

In this study, we demonstrated that compared to OA alone, the changes of OPOA subchondral bone mainly take place in cancellous bone. While the area change of trabecular bone was significantly different between the two groups, no statistical difference was observed in cortical bone. It is possible that the abnormal reconstruction of subchondral bone in the early OPOA is chiefly manifested in a change in trabecular bone. In addition, we characterized trabecular bone below the growth plate, in which the OVX mice exhibited a significant decrease in trabecular bone but no significant change was detected between the sham and the simple OA groups. Therefore, knee loading may mainly play a role in the regulation of trabecular bone.

This study has limitations. We employed small animals, but the responses in large animals or human subjects may differ. In particular, the beneficial loading condition was based on small animals, and it is necessary to re-evaluate proper loading conditions for large animals or human subjects. Our results show that OP aggravates the symptoms of the early OA based on bone loss on subchondral bone. However, the effect of OP on the symptoms of advanced OA is unclear and needs further study.

In summary, this study demonstrates that knee loading is effective in increasing SBP and B.Ar/T.Ar, decreasing OARSI score and CC/TAC in OA and OPOA mice. The results show that in OPOA, knee loading can prevent cartilage degradation and regulate subchondral bone remodeling by promoting osteoblast formation and suppressing abnormal osteoclast activity. Therefore, knee loading could offer a new non-invasive strategy for OPOA treatment. Further studies should be performed to clarify the influence of OP on advanced OA and the therapeutic effect of knee loading.

ACKNOWLEDGMENTS

This work was supported by grant from National Natural Science Foundation of China (81572100 and 81772405 to P. Zhang; 81601863 to X. Li), Natural Science Foundation of Tianjin (18JCQNJC82200 to X. Li), and NIH (AR052144 to H. Yokota).

ABBREVIATIONS:

ALP	alkaline phosphatase
B.Ar/T.Ar	subchondral bone volume fraction
BMC	bone mineral content
BMD	bone mineral density
BMSCs	bone marrow mesenchymal stem cells
BV/TV	bone volume fraction

CC/TAC	ratio of calcified cartilage to total articular cartilage
CTSK	cathepsin K
FV	field of vision
H&E	hematoxylin and eosin
M-CSF	macrophage-colony stimulating factor
N.Ob/BS	osteoblast number/bone surface
OA	osteoarthritis
OARSI	osteoarthritis research society international
Oc.S/BS	osteoclast surface/bone surface
OP	osteoporosis
OPOA	osteoporotic osteoarthritis
RANKL	receptor activator of nuclear factor kappa-B ligand
RUNX2	runt-related transcription factor 2
SBP	subchondral bone plate
TRAP	tartrate resistant acid phosphatase
Wnt	wingless/integrated

REFERENCES

1. Black DM, and Rosen CJ (2016) Clinical practice. Postmenopausal osteoporosis. N. Engl. J. Ned 374, 254–262
2. Loeser RF, Collins JA, and Diekman BO (2016) Ageing and the pathogenesis of osteoarthritis. Nat. Rev. Rheumatol 12, 412–420 [PubMed: 27192932]
3. Compston JE, McClung MR, and Leslie WD (2019) Osteoporosis. Lancet 393, 364–376 [PubMed: 30696576]
4. Roman-Blas JA, and Herrero-Beaumont G (2014) Targeting subchondral bone in osteoporotic osteoarthritis. Arthritis Res. Ther 16, 494 [PubMed: 25664969]
5. Herrero-Beaumont G, and Roman-Blas JA (2013) Osteoporotic OA: a reasonable target for bone-acting agents. Nat. Rev. Rheumatol 9, 448–450 [PubMed: 23857129]
6. Im GI, and Kim MK (2014) The relationship between osteoarthritis and osteoporosis. J. Bone Miner. Metab 32, 101–109 [PubMed: 24196872]
7. Bijlsma JWJ, Berenbaum F, and Lafeber FPJG (2011) Osteoarthritis: an update with relevance for clinical practice. Lancet 377, 2115–2126 [PubMed: 21684382]
8. Bultink IE, and Lems WF (2013) Osteoarthritis and osteoporosis: what is the overlap? Curr. Rheumatol. Rep 15, 328 [PubMed: 23508809]
9. Li G, Yin J, Gao J, Cheng TS, Pavlos NJ, Zhang C, and Zheng MH (2013) Subchondral bone in osteoarthritis: insight into risk factors and microstructural changes. Arthritis Res. Ther 15, 223 [PubMed: 24321104]
10. Iijima H, Aoyama T, Tajino J, Ito A, Nagai M, Yamaguchi S, Zhang X, Kiyan W, and Kuroki H (2016) Subchondral plate porosity colocalizes with the point of mechanical load during ambulation

in a rat knee model of post-traumatic osteoarthritis. Osteoarthritis Cartilage 24, 354–363 [PubMed: 26376125]

11. Neogi T, Nevitt M, Niu J, Sharma L, Roemer F, Guermazi A, Lewis CE, Torner J, Javaid K, and Felson D (2010) Subchondral bone attrition may be a reflection of compartment-specific mechanical load: the MOST Study. Ann. Rheum. Dis 69, 841–844 [PubMed: 19762366]
12. Li X, Lang W, Ye H, Yu F, Li H, Chen J, Cai L, Chen W, Lin R, Huang Y, and Liu X (2013) Tougu Xiaotong capsule inhibits the tidemark replication and cartilage degradation of papain-induced osteoarthritis by the regulation of chondrocyte autophagy. Int. J. Mol. Med 31, 1349–1356 [PubMed: 23589102]
13. Lv H, Zhang L, Yang F, Zhao Z, Yao Q, Zhang L, and Tang P (2015) Comparison of microstructural and mechanical properties of trabeculae in femoral head from osteoporosis patients with and without cartilage lesions: a case-control study. BMC. Musculoskelet. Disord 16, 72 [PubMed: 25887431]
14. Kodri K, Zupan J, Kranjc T, Komadina R, Mlakar V, Marc J, and Lovšin N (2019) Sex-determining region Y (SRY) attributes to gender differences in RANKL expression and incidence of osteoporosis. Exp. Mol. Med 51,(8):97 [PubMed: 31409771]
15. Lotinun S, Ishihara Y, Nagano K, Kiviranta R, Carpentier VT, Neff L, Parkman V, Ide N, Hu D, Dann P, Brooks D, Bouxsein ML, Wysolmerski J, Gori F, and Baron R (2019) Cathepsin K-deficient osteocytes prevent lactation-induced bone loss and parathyroid hormone suppression. J. Clin. Invest129, 3058–3071 [PubMed: 31112135]
16. Park OJ, Kim J, Yang J, Yun CH, and Han SH (2019) Muramyl dipeptide, a shared structural motif of peptidoglycans, is a novel inducer of bone formation through induction of RUNX2. J. Bone Miner. Res 34,(5):975 [PubMed: 31132318]
17. Zhang P, and Yokota H (2012) Elbow loading promotes longitudinal bone growth of the ulna and the humerus. J. Bone Miner. Metab 30, 31–39 [PubMed: 21748461]
18. Liu D, Li X, Li J, Yang J, Yokota H, and Zhang P (2015) Knee loading protects against osteonecrosis of the femoral head by enhancing vessel remodeling and bone healing. Bone 81, 620–631 [PubMed: 26416150]
19. Zhang P, Turner CH, and Yokota H (2009) Joint loading-driven bone formation and signaling pathways predicted from genome-wide expression profiles. Bone 44, 989–998 [PubMed: 19442616]
20. Yang S, Liu H, Zhu L, Li X, Liu D, Song X, Yokota H, and Zhang P (2019) Ankle loading ameliorates bone loss from breast cancer-associated bone metastasis. FASEB J fj201900306RR [Epub ahead of print]
21. Zhang P, Su M, Liu Y, Hsu A, and Yokota H (2007) Knee loading dynamically alters intramedullary pressure in mouse femora. Bone 40, 538–543 [PubMed: 17070127]
22. Zhang P, and Yokota H (2011) Knee loading stimulates healing of mouse bone wounds in a femur neck. Bone 49, 867–872 [PubMed: 21723427]
23. Li X, Liu D, Li J, Yang S, Xu J, Yokota H, and Zhang P (2019) Wnt3a involved in the mechanical loading on improvement of bone remodeling and angiogenesis in a postmenopausal osteoporosis mouse model. FASEB J. 33(8):8913–8924. [PubMed: 31017804]
24. Zheng W, Li X, Liu D, Li J, Yang S, Gao Z, Wang Z, Yokota H, and Zhang P (2019) Mechanical loading mitigates osteoarthritis symptoms by regulating endoplasmic reticulum stress and autophagy. FASEB J 33, 4077–4088 [PubMed: 30485126]
25. Li X, Yang J, Liu D, Li J, Niu K, Feng S, Yokota H, and Zhang P (2016) Knee loading inhibits osteoclast lineage in a mouse model of osteoarthritis. Sci. Rep 6, 24668 [PubMed: 27087498]
26. Baron R, and Kneissel M (2013) Wnt signaling in bone homeostasis and disease: from human mutations to treatments. Nat. Med 19, 179–192 [PubMed: 23389618]
27. Zhong Z, Zylstra-Diegel CR, Schumacher CA, Baker JJ, Carpenter AC, Rao S, Yao W, Guan M, Helms JA, Lane NE, Lang RA, and Williams BO (2012) Wntless functions in mature osteoblasts to regulate bone mass. Proc. Natl. Acad. Sci. U. S. A 109, E2197–2204 [PubMed: 22745162]
28. Lerner UH, and Ohlsson C (2015) The Wnt system: background and its role in bone. J. Intern. Med 277, 630–649 [PubMed: 25845559]

29. Lara-Castillo N, Kim-Weroha NA, Kamel MA, Javaheri B, Ellies DL, Krumlauf RE, Thiagarajan G, and Johnson ML (2015) In vivo mechanical loading rapidly activates beta-catenin signaling in osteocytes through a prostaglandin mediated mechanism. Bone 76, 58–66 [PubMed: 25836764]
30. Javaheri B, Stern AR, Lara N, Dallas M, Zhao H, Liu Y, Bonewald LF, and Johnson ML (2014) Deletion of a single beta-catenin allele in osteocytes abolishes the bone anabolic response to loading. J. Bone Miner. Res 29, 705–715 [PubMed: 23929793]
31. Hamamura K, Zhang P, Zhao L, Shim JW, Chen A, Dodge TR, Wan Q, Shih H, Na S, Lin CC, Sun HB, and Yokota H (2013) Knee loading reduces MMP13 activity in the mouse cartilage. BMC. Musculoskelet. Disord 14, 312 [PubMed: 24180431]
32. Wang CJ, Huang CY, Hsu SL, Chen JH, and Cheng JH (2014) Extracorporeal shockwave therapy in osteoporotic osteoarthritis of the knee in rats: an experiment in animals. Arthritis Res. Ther 16, R139 [PubMed: 24994452]
33. Shuai B, Shen L, Yang Y, Ma C, Zhu R, and Xu X (2015) Assessment of the Impact of Zoledronic Acid on Ovariectomized Osteoporosis Model Using Micro-CT Scanning. PLoS One 10, e0132104 [PubMed: 26148020]
34. Tan N, Li X, Zhai L, Liu D, Li J, Yokota H, and Zhang P (2018) Effects of knee loading on obesity-related non-alcoholic fatty liver disease in an ovariectomized mouse model with high-fat diet. Hepatol. Res 48, 839–849. [PubMed: 29601135]
35. Zhen G, Wen C, Jia X, Li Y, Crane JL, Mears SC, Askin FB, Frassica FJ, Chang W, Yao J, Carrino JA, Cosgarea A, Artemov D, Chen Q, Zhao Z, Zhou X, Riley L, Sponseller P, Wan M, Lu WW, and Cao X (2013) Inhibition of TGF-β signaling in mesenchymal stem cells of subchondral bone attenuates osteoarthritis. Nat. Med 19, 704–712 [PubMed: 23685840]
36. Glasson SS, Chambers MG, Van Den Berg WB, and Little CB (2010) The OARSI histopathology initiative - recommendations for histological assessments of osteoarthritis in the mouse. Osteoarthritis Cartilage 18 Suppl 3, S17–23
37. Moskowitz RW (2006) Osteoarthritis cartilage histopathology: grading and staging. Osteoarthritis Cartilage 14, 1–2 [PubMed: 16242362]
38. Kim JH, Jeon J, Shin M, Won Y, Lee M, Kwak JS, Lee G, Rhee J, Ryu JH, Chun CH, and Chun JS (2014) Regulation of the catabolic cascade in osteoarthritis by the zinc-ZIP8-MTF1 axis. Cell 156, 730–743 [PubMed: 24529376]
39. Wu X, Chen S, He Y, Rhodes SD, Mohammad KS, Li X, Yang X, Jiang L, Nalepa G, Snider P, Robling AG, Clapp DW, Conway SJ, Guise TA, and Yang FC (2011) The haploinsufficient hematopoietic microenvironment is critical to the pathological fracture repair in murine models of neurofibromatosis type 1. PLoS One 6, e24917 [PubMed: 21980365]
40. Sharma R, Wu X, Rhodes SD, Chen S, He Y, Yuan J, Li J, Yang X, Li X, Jiang L, Kim ET, Stevenson DA, Viskochil D, Xu M, and Yang FC (2013) Hyperactive Ras/MAPK signaling is critical for tibial nonunion fracture in neurofibromin-deficient mice. Hum. Mol. Genet 22, 4818–4828 [PubMed: 23863460]
41. Wang H, and Liu D (2014) Baicalin inhibits high-mobility group box 1 release and improves survival in experimental sepsis. Shock 41, 324–330 [PubMed: 24430548]
42. Yokota H, Hamamura K, Chen A, Dodge TR, Tanjung N, Abedinpoor A, and Zhang P (2013) Effects of salubrinal on development of osteoclasts and osteoblasts from bone marrow-derived cells. BMC. Musculoskelet. Disord 14, 197 [PubMed: 23816340]
43. Mussazhanova Z, Akazawa Y, Matsuda K, Shichijo K, Miura S, Otsubo R, Oikawa M, Yoshiura K, Mitsutake N, Rogounovitch T, Saenko V, Kozykenova Z, Zhetpisbaev B, Shabdarbaeva D, Sayakenov N, Amantayev B, Kondo H, Ito M, and Nakashima M (2016) Association between p53-binding protein 1 expression and genomic instability in oncocytic follicular adenoma of the thyroid. Endocr. J 63, 457–467 [PubMed: 26935218]
44. Xiao G, Cheng H, Cao H, Chen K, Tu Y, Yu S, Jiao H, Yang S, Im HJ, Chen D, Chen J, and Wu C (2012) Critical role of filamin-binding LIM protein 1 (FBLP-1)/migfilin in regulation of bone remodeling. J. Biol. Chem 287, 21450–21460 [PubMed: 22556421]
45. Li C, Sunderic K, Nicoll SB, and Wang S (2018) Downregulation of heat shock protein 70 impairs osteogenic and chondrogenic differentiation in human mesenchymal stem cells. Sci. Rep 8, 553 [PubMed: 29323151]

46. Castaneda S, Largo R, Calvo E, Rodriguez-Salvanes F, Marcos ME, Diaz-Curiel M, and Herrero-Beaumont G (2006) Bone mineral measurements of subchondral and trabecular bone in healthy and osteoporotic rabbits. Skeletal. Radiol 35, 34–41 [PubMed: 16247642]

47. Dequeker J, Aerssens J, and Luyten FP (2003) Osteoarthritis and osteoporosis: clinical and research evidence of inverse relationship. Aging Clin. Exp. Res 15, 426–439 [PubMed: 14703009]

48. Goldring MB, and Goldring SR (2010) Articular cartilage and subchondral bone in the pathogenesis of osteoarthritis. Ann. N. Y. Acad. Sci 1192, 230–237 [PubMed: 20392241]

49. Holopainen JT, Brama PA, Halmesmäki E, Harjula T, Tuukkanen J, van Weeren PR, Helminen HJ, and Hyttinen MM (2008) Changes in subchondral bone mineral density and collagen matrix organization in growing horses. Bone 43, 1108–1114 [PubMed: 18757048]

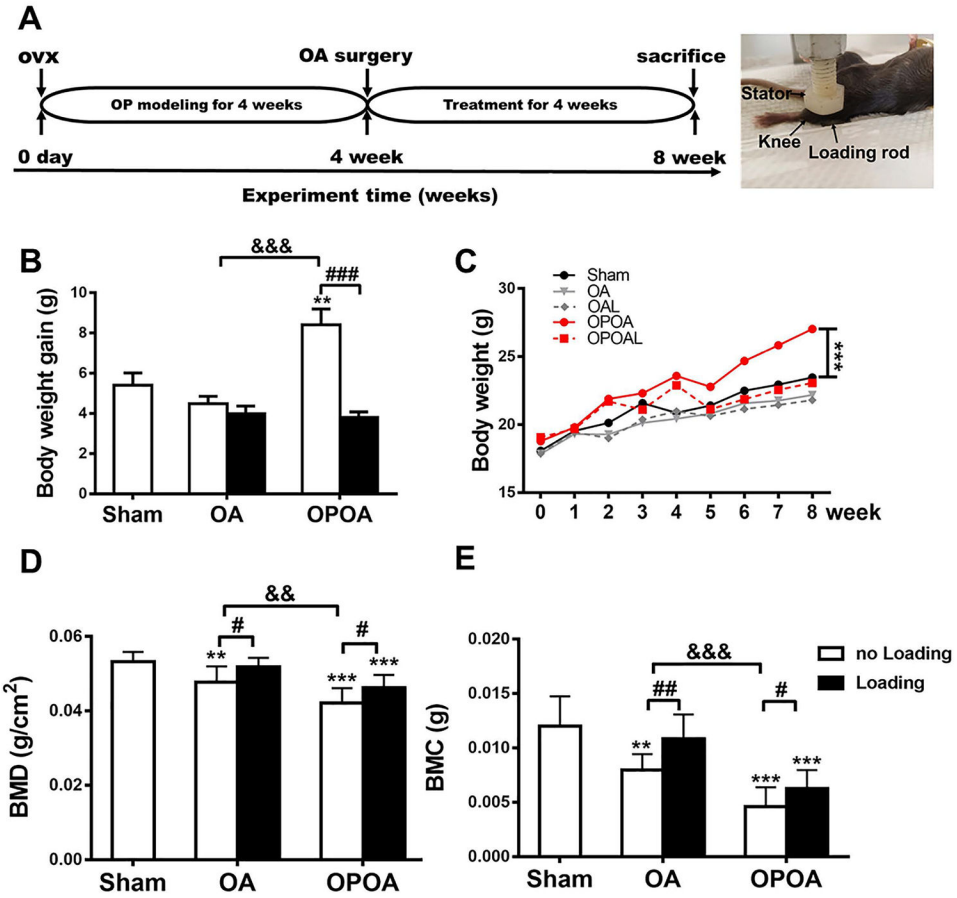

Fig. 1. Experimental timeline, setting of knee loading and the effect of knee loading on body weight and bone mass.

A) Experimental timeline (left) and loading site for knee loading (right, Bar = 1 cm). *B, C*) Effects of knee loading on body weight gain (*B*) and body weight (*C*) in OPOA mice, recorded weekly during the experimental period. *D, E*) Effects of knee loading on BMD (*D*) and BMC (*E*) *in vivo*. The data were expressed with standard deviation (SD). n = 16 per group. ** = $P < 0.01$ and *** = $P < 0.001$ vs sham group; # = $P < 0.05$, ## = $P < 0.01$ and ### = $P < 0.001$; && = $P < 0.01$ and &&& = $P < 0.001$.

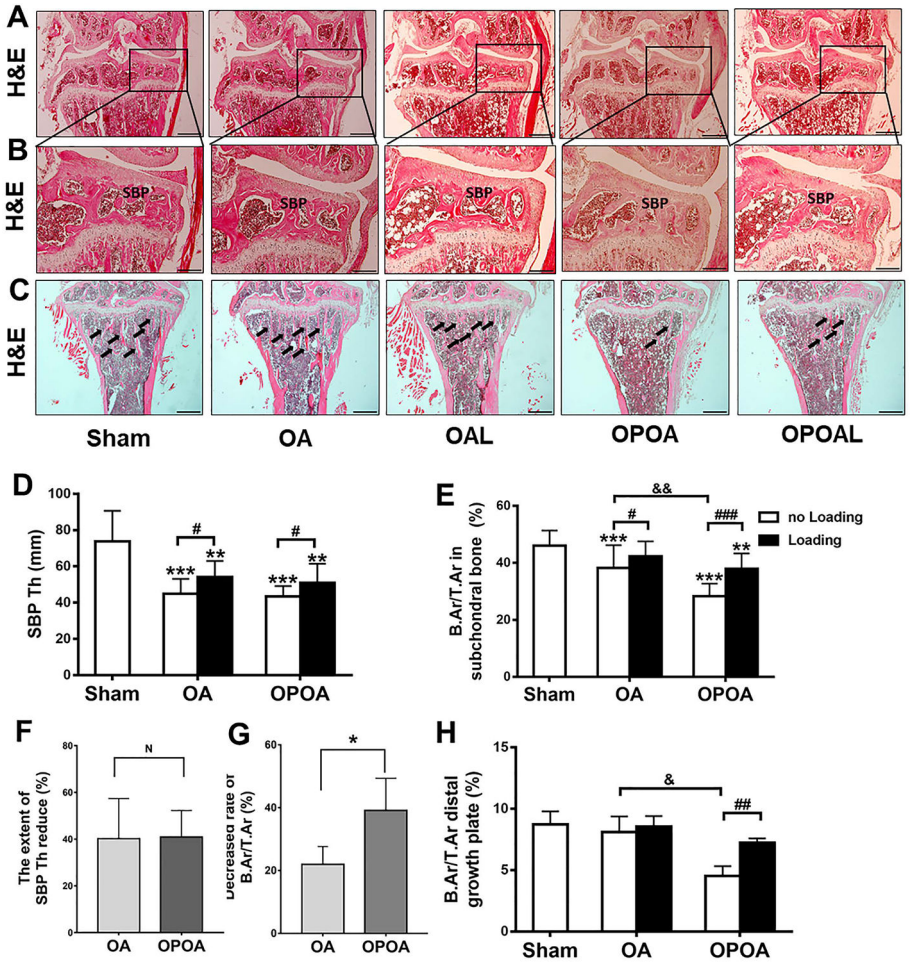

Fig. 2. Effect of knee loading on subchondral bone and cancellous bone under the growth plate.

A-E) Representative H&E-stained images *A-C*) and quantification of thickness of SBP (SBP.Th) (*D*) and B.Ar/T.Ar (E). *F, G*) Changes in cortical (*F*) and cancellous bone (*G*). *H*) Quantification of B.Ar/T.Ar under the growth plate. n = 10 per group. ** = $P < 0.01$ and *** = $P < 0.001$ vs sham group; # = $P < 0.05$, ## = $P < 0.01$ and ### = $P < 0.001$; && = $P < 0.01$. D and E were expressed with standard deviation (SD).

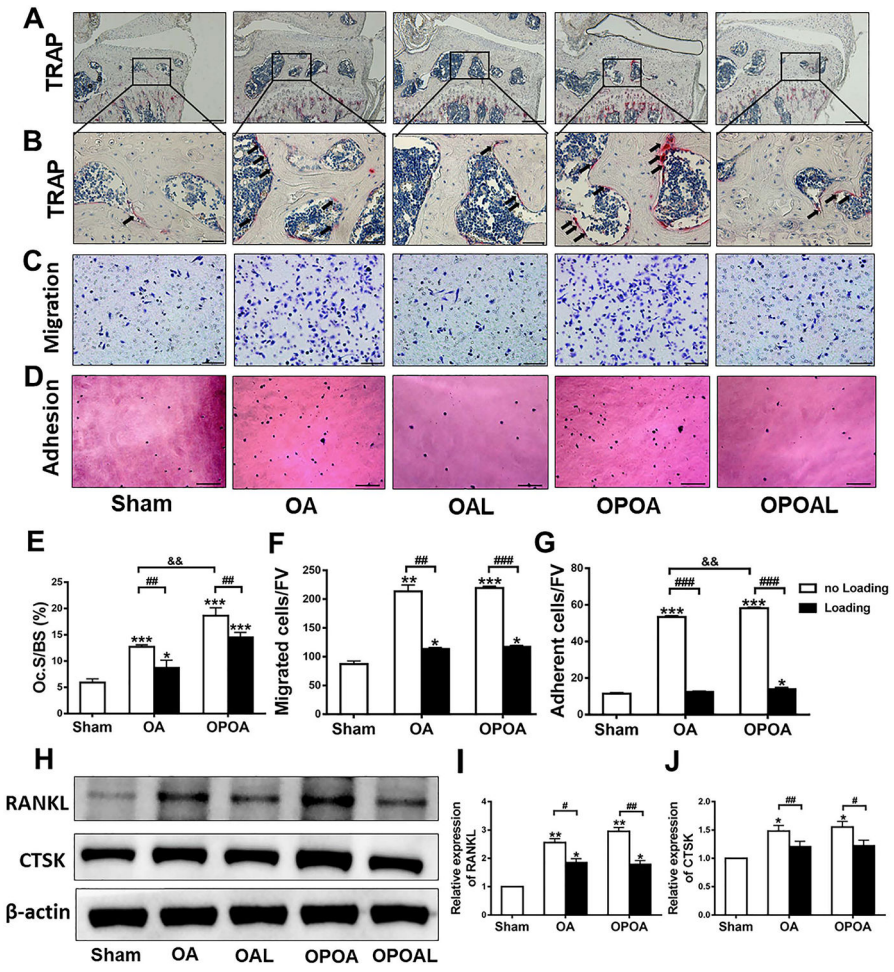

Fig. 3. Effect of knee loading on osteoclast development.

A, B) TRAP staining was used to evaluate bone resorption, Bar = 200 μm (*A*) and Bar = 50 μm (*B*). TRAP-positive cells, red color, indicated by the arrows. *C-D*) Effects of knee loading on osteoclast migration (*C*) and adhesion (*D*), Bar = 200 μm. *E-G*) Quantification of TRAP-positive cells (*E*), osteoclast migration (*F*) and adhesion (*G*). *H-J*) Western blot (*H*) showed the protein level of RANKL and CTSK and relative quantification of protein level of RANKL (*I*) and CTSK (*J*). n = 3 per group. * = $P < 0.05$, ** = $P < 0.01$ and *** = $P < 0.001$ vs sham group; # = $P < 0.05$, ## = $P < 0.01$ and ### = $P < 0.001$; && = $P < 0.01$.

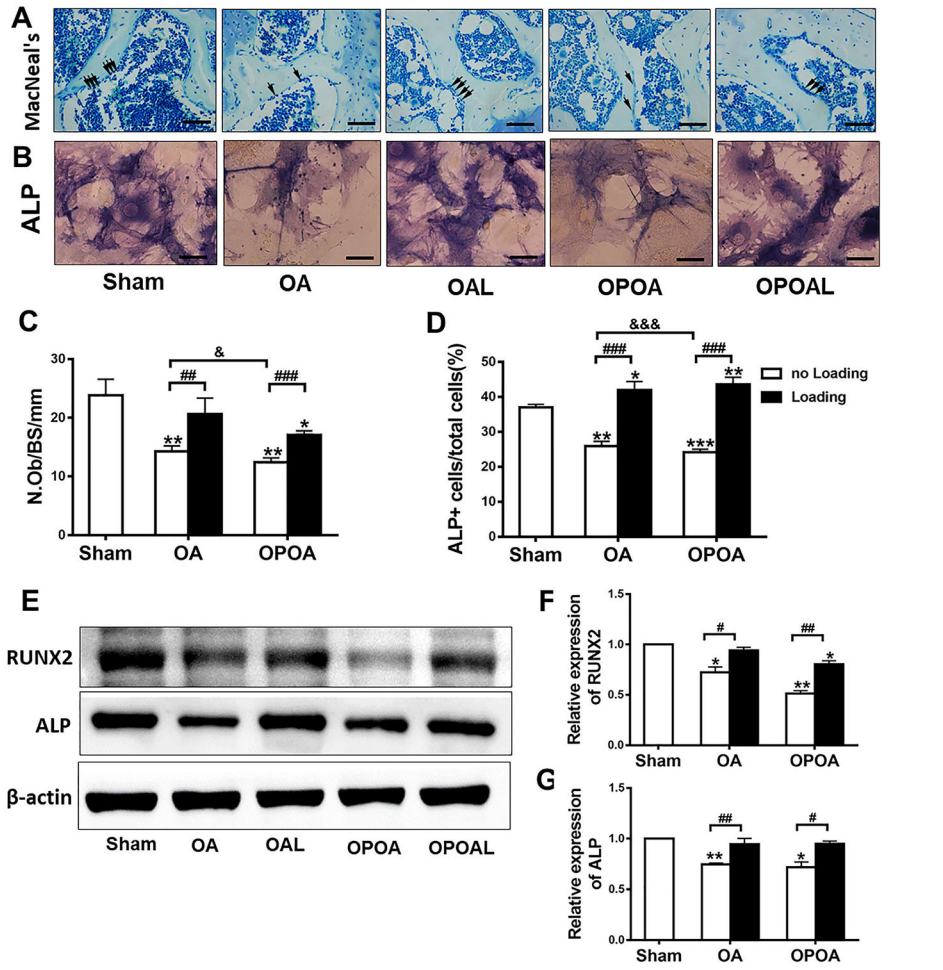

Fig. 4. Effect of knee loading on differentiation of osteoblast.

A-D) MacNeal's staining was used to identify osteoblasts, Bar = 50 μm (*A*). Osteoblasts, located on trabecular surface, were indicated by the arrows. Bone marrow-derived cells were cultured in 6-well plates for 14 days, ALP staining was used to detect osteoblast differentiation, Bar = 50 μm (*B*). The number of osteoblasts were counted (*C*) and the ratio of the numbers of ALP-positive cells to that of total cells was determined (*D*). *E-G*) Western blot (*E*) showed the protein level of RUNX2 and ALP and relative quantification of protein level of RUNX2 (*F*) and ALP (*G*). n = 3 per group. * = $P < 0.05$, ** = $P < 0.01$ and *** = $P < 0.001$ vs sham group; # = $P < 0.05$, ## = $P < 0.01$ and ### = $P < 0.001$; & = $P < 0.05$ and &&& = $P < 0.001$.

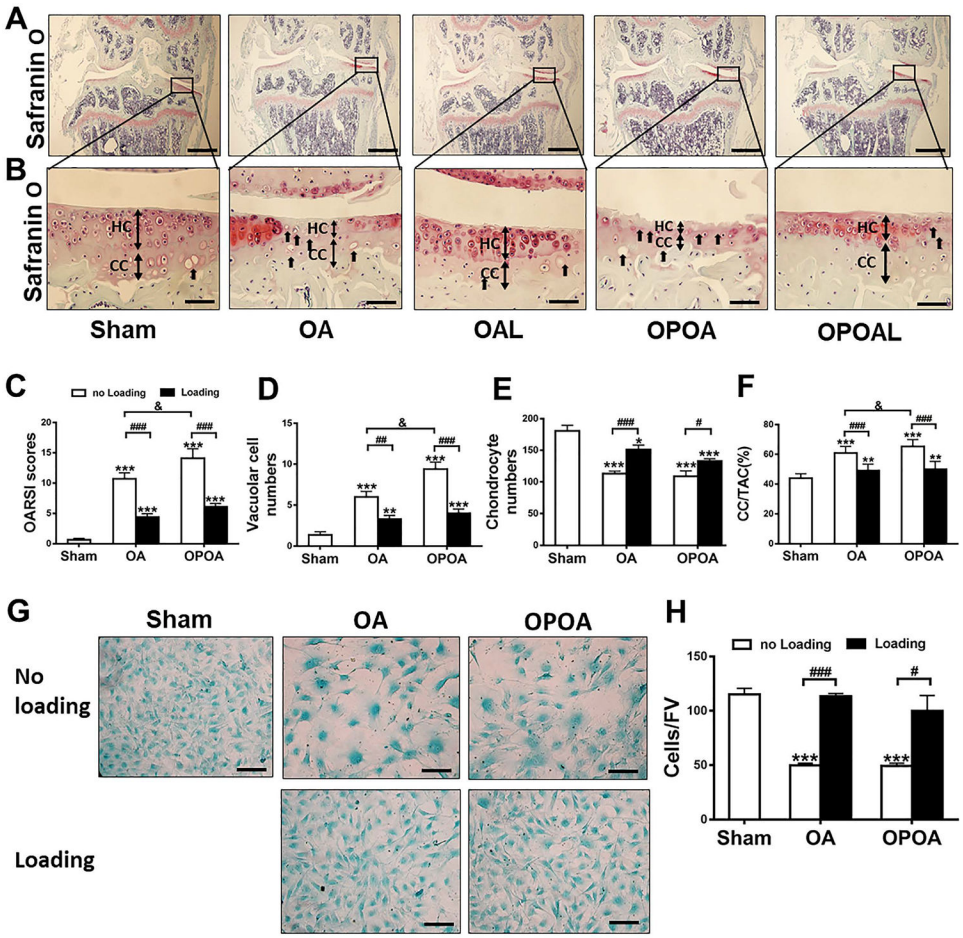

Fig. 5. Knee loading protected articular cartilage from damage and increases the number of chondrocytes.

A-F) Representative Safranin O–stained images (*A-B*) and quantification of OARSI scores (*C*), vacuolar cell (*D*), Chondrocyte (*E*) numbers and the value of CC/TAC (*F*) in area proximal to subchondral bone of medial tibial plateau. Black arrows indicate vacuolar cells (*B*), Bar = 500 μm (*A*) and Bar = 50 μm (*B*), n = 10 per group. *G, H*) Representative images of chondrocyte from mouse-derived bone mesenchymal cells (G) and quantification of chondrocyte numbers (H). n = 3 per group. * = $P < 0.05$, ** = $P < 0.01$ and *** = $P < 0.001$ vs sham group; # = $P < 0.05$, ## = $P < 0.01$ and ### = $P < 0.001$; & = $P < 0.05$.

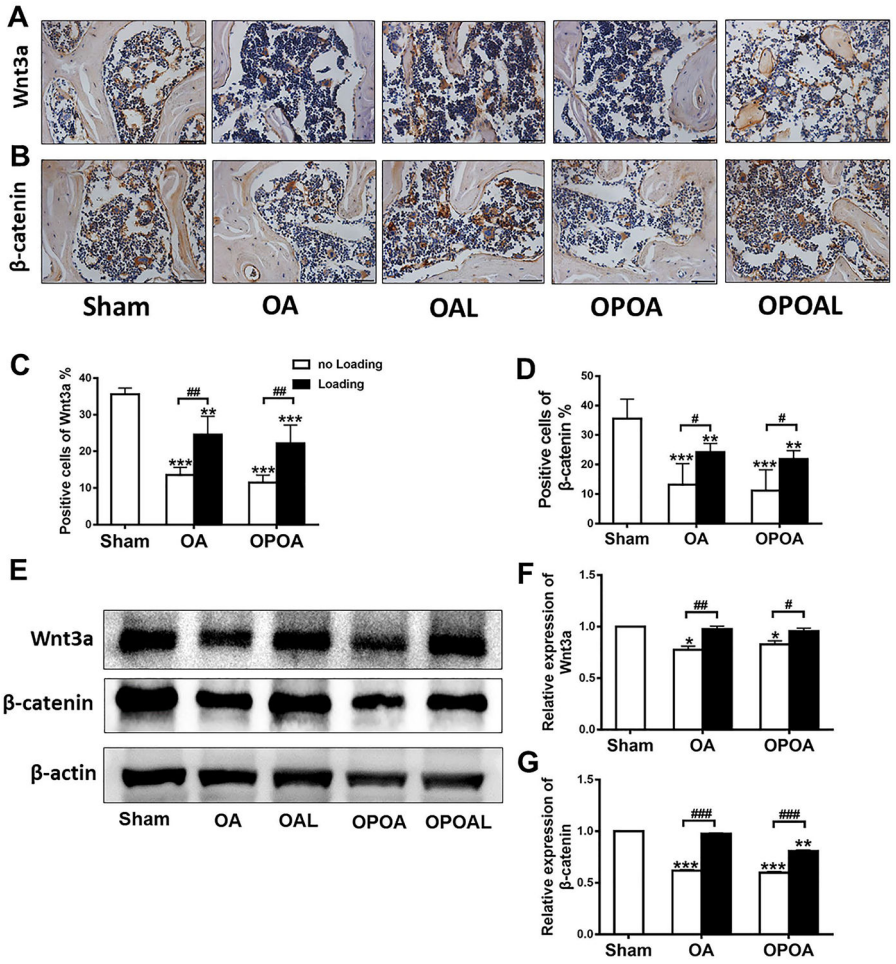

Fig. 6. Knee loading increased the expression of Wnt3a and β-catenin in the OAL and OPOAL groups.

A, B) Immunohistochemistry staining of Wnt3a (*A*) and β-catenin (*B*) in coronal sections of Subchondral bone were conducted, Bar = 50μm. *C, D*) Quantification of Wnt3a (*C*) and β-catenin (*D*) positive cells in Subchondral bone were examined. *E-G*) Western blot (*E*) showed the protein level of Wnt3a and β-catenin and relative quantification of protein level of Wnt3a (*F*) and β-catenin (*G*). n = 3 per group. * = $P < 0.05$, ** = $P < 0.01$ and *** = $P < 0.001$ vs sham group; # = $P < 0.05$, ## = $P < 0.01$ and ### = $P < 0.001$.

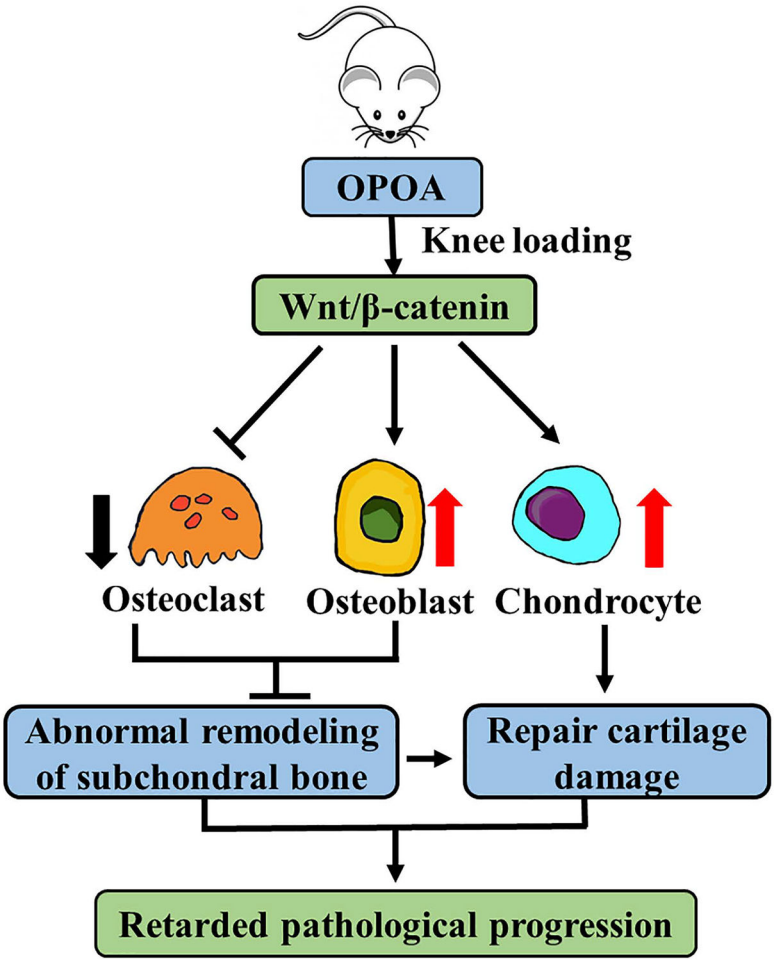

Fig. 7.

Mechanism of knee loading that mitigates OPOA symptoms by relieving subchondral bone abnormal remodeling through regulate Wnt/β-catenin signaling.